A Final Technical Report on
Clutter Rejection for Mid Infrared
Surveillance

Contract with Naval Research Laboratory
Washington, D.C.   20375
Contract No. N00014-82-K-2009

OGDEN COLLEGE OF SCIENCE, TECHNOLOGY AND HEALTH

WESTERN KENTUCKY UNIVERSITY
Bowling Green, Kentucky 42101

DTIC
ELECTE
FEB 1   1984

A

84 01 09 009

A Final Technical Report on
Clutter Rejection for Mid Infrared
Surveillance

Contract with Naval Research Laboratory
Washington, D.C. 20375
Contract No. N00014-82-K-2009

1983

A

A Final Technical Report on
Clutter Rejection for Mid Infrared Surveillance
Contract with Naval Research Laboratory
Washington, D.C.   20375
Contract No. N00014-82-K-2009

Contractor
Western Kentucky University
Office of Sponsored Programs
Bowling Green, Kentucky   42101

Project Director
Dr. Martin S. Longmire
Department of Physics and Astronomy
Western Kentucky University
Bowling Green, Kentucky   42101

Copies to: NRL 6550
NRL 6502
NRL 2415
NRL 2627
DDC
ONR, Columbus, Ohio

Required forms for project close-out will be filed
with the Final Financial Report.

CONTENTS

INTRODUCTION

This report is in four parts. The first part is an article presented at the February 1983 meeting of the IRIS Specialty Group on Targets, Backgrounds, and Discrimination. Since the text is classified CONFIDENTIAL, it is not included here. Instead the article is represented by a page giving the unclassified title, the authors, and a reference to the symposium proceedings where the text can be found.

The work leading to the IRIS article uncovered deficiencies in the methods of manipulating recorded clutter data to study the effect of spatial resolution on clutter rejection and signal detection. The second part of this report notes the deficiencies and indicates whether and how they can be corrected. One of the correction techniques will be described in a future article after it has been tested and proven by computations.

Part 3 is an article which reports the results of studies to elucidate the operation of an adaptive threshold sensor and to determine how its size affects signal detection. This article has been submitted for publication in the journal, Applied Optics.

Finally, part 4 summarizes work done to obtain data suitable for simulating two-dimensional signal processing.

PART 1

Simulation of Cloud Clutter Rejection by Spatial
Discrimination and Threshold Detection (U)

A. F. Milton, M. S. Longmire, and E. H. Takken

A classified article (CONFIDENTIAL) published in
Proceedings of the IRIS Specialty Group on Targets,
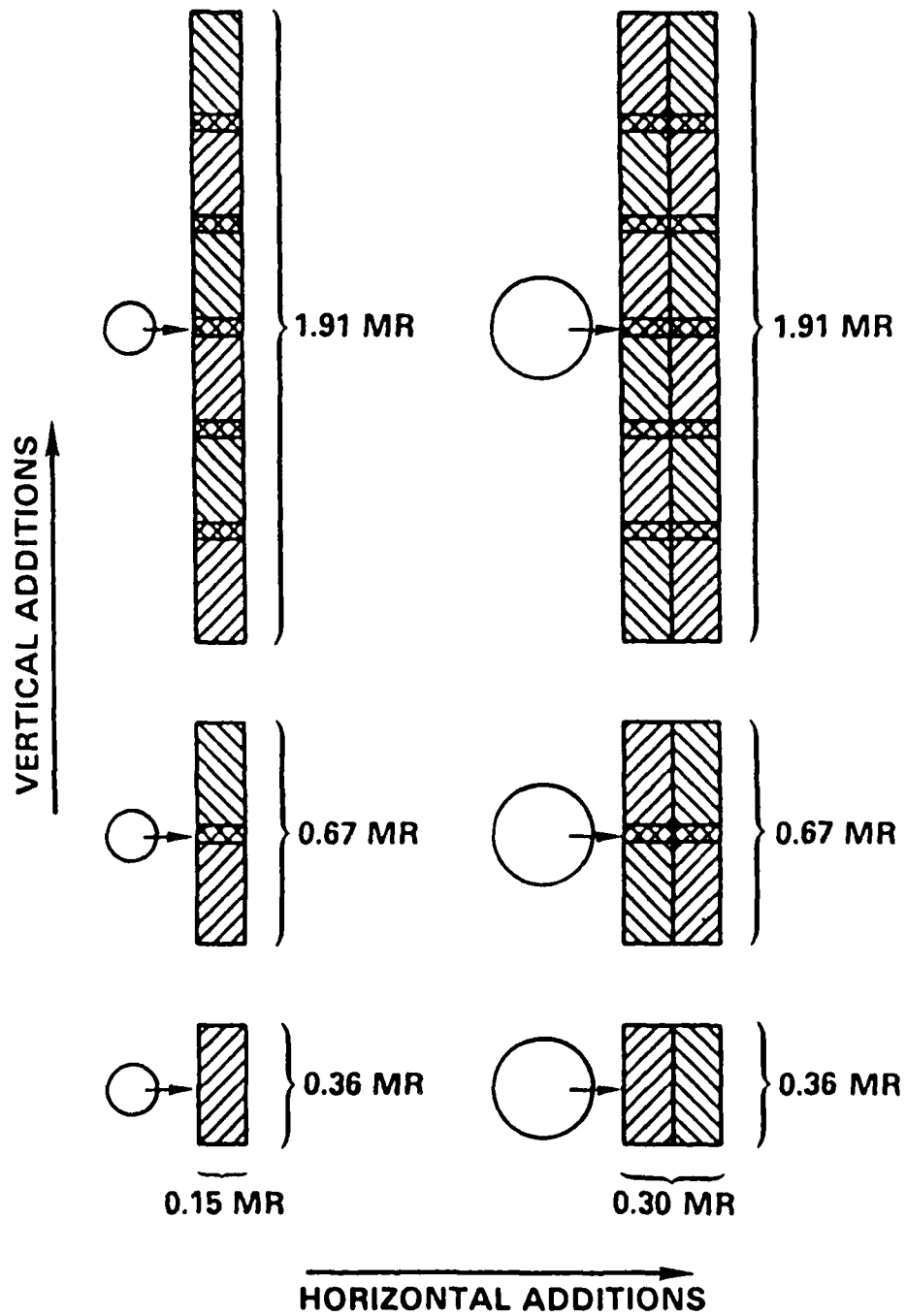Backgrounds, and Discrimination, February 1983.

PART 2

Problems Associated with Changing the Spatial Resolution
of Recorded Clutter Data

In the IRIS article of part 1, the spatial resolution of recorded clutter data was degraded in order to study the role of spatial resolution in clutter rejection and signal detection. The procedures employed are indicated schematically in Figure 2.1. Degradation in the cross-scan (vertical) direction requires only aligning the channels and adding sampled values from them, effectively increasing the pixel (detector) height. Degradation in the scan (horizontal) direction requires increasing the detector width by summing adjacent pixels. It is usually desirable to perform another summation which increases the blur circle size keeping it matched to the detector width, since this is the way most optical sensors are made.

These summations involve a number of difficulties. First, unless the sampling rate is chosen very carefully, the channels cannot be aligned exactly, and horizontal pixels overlap when added. Provided sampling is instantaneous, these problems can be overcome by interpolating the data with a cardinal function and summing the interpolated data. Second, the detector noise (from photon fluctuations and the usual sources in the detector and electronics) is increased by the pixel summations. Third, detector elements in staggered columns may overlap vertically as in Figure 2.1 leading to areas of doubled sensitivity in the new pixels. Neither of these problems can be corrected because clutter is a super-position of two components, random detector noise and deterministic pure

Figure 2.1

RESOLUTION CHANGES

1.91 MR

1.91 MR

VERTICAL ADDITIONS

0.67 MR

0.67 MR

0.36 MR

0.36 MR

0.15 MR

0.30 MR

HORIZONTAL ADDITIONS

clutter noise from the non-uniform background radiance. One can think of techniques for correcting either component at least partially, but the methods are different for the two components and cannot be applied to them separately. Finally, the summations which increase detector size and blur circle size represent optical linear filtering. Figure 2.2 shows the amplitude response of the optical degradation filter used in the IRIS article of part 1 and, for comparison, the amplitude response of the associated 1-D LMS filter. With recorded data the degradation filter acts on both the pure clutter and the detector noise altering the frequency dependence of their power spectra, properly for the pure clutter, but improperly for the detector noise since its frequency content cannot actually be affected by optical filtering. This problem can be corrected approximately by adding back the part of the detector noise improperly removed by the optical degradation filter. A method for doing this has been worked out and will be published after it has been tested and proven by calculations.

Figure 2.2

LMS VS RESOLUTION BROADENING FILTER
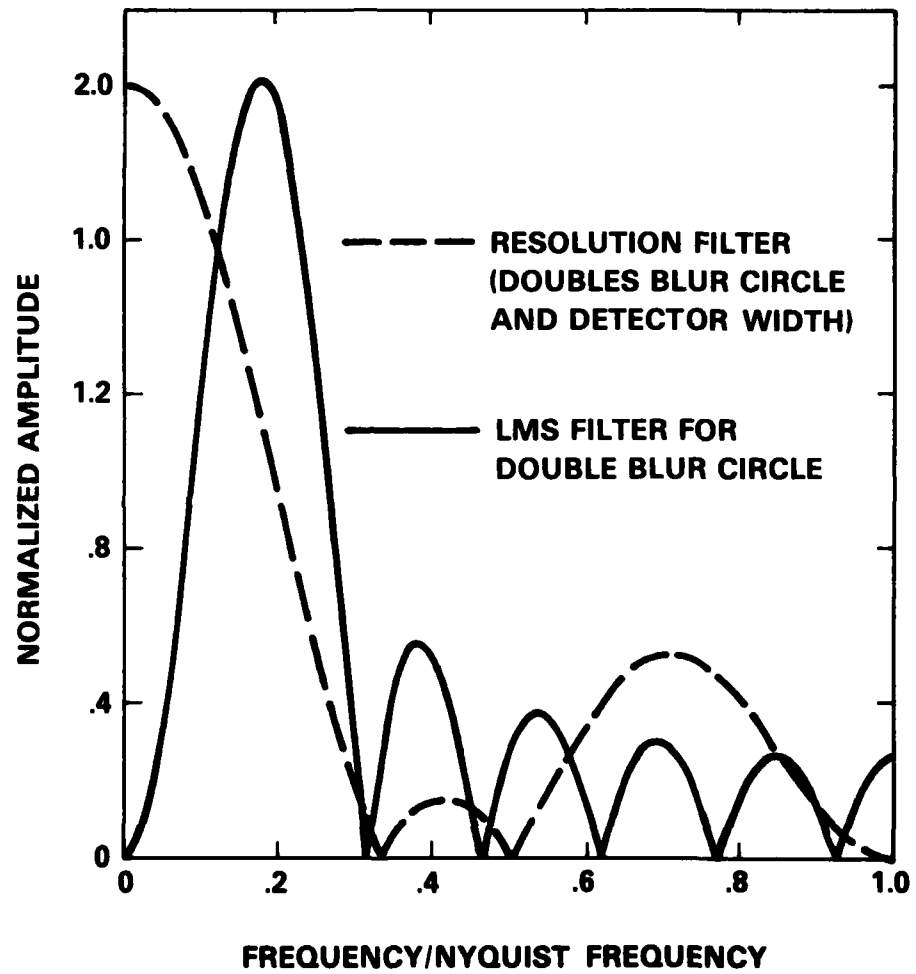
PART 3

Simulation of Mid-Infrared Clutter Rejection. 2: Threshold-sensor
Size-effects with LMS-filtered Noise

M. S. Longmire, F. D. Bryant, J. D. Wilkey, and A. F. Milton

Abstract

The relation between an adaptive threshold sensor's size and its performance is analyzed numerically using LMS-filtered noise. The analysis links signal detection to size through the threshold parameter, sampling variance, and a "clutter-edge effect," with account taken of non-random sampling, correlation, and non-stationarity of the noise. A principle is established for determining whether a 2-D threshold sensor is advantageous; it is not under the conditions of this simulation. Critical, optimum, and best sizes are given for a 1-D threshold sensor following a 1-D LMS filter with input from an optical sensor having NEI (noise equivalent irradiance) = 1.5×10^{-13} W/cm^2 and spatial resolution 0.15×0.36 milliradians.

1. Introduction

This article, like the first one, discusses simulation of cloud clutter rejection using recorded natural background noise and algorithms programmed for a digital computer to represent components of a mid-IR surveillance set. The background data, the algorithms, and the method of simulation are described in the first article, which compares the performance of two threshold sensors - one fixed, the other adaptive - following several 1-D linear filters.[1] The combination of a 1-D adaptive threshold sensor and a 1-D LMS spatial filter suppresses extreme cloud clutter effectively and detects simlulated signals almost as well in clutter as in uniform sky. It was noted in the first article that the performance of an adaptive threshold sensor depends on its size (its spatial extent or the number of background data used to estimate the local noise statistics), but only one size was studied previously. Here we report results of further work to determine how changing the size of a 1-D threshold sensor following a 1-D LMS filter affects signal detection. We also present a numerical analysis of the threshold sensor's sampling performance, taking account of non-random sampling, correlation, and non-stationarity of the LMS-filtered noise. This leads to some useful experimental generalizations and to a principle for determining whether a 2-D threshold sensor is advantageous. The method of analysis is applicable wherever recorded background data are available and should be useful for developing threshold sensors to operate under conditions different from the ones in this simulation.

II. Results and Discussion

The quality of signal detection achieved with an adaptive threshold sensor depends on the average threshold $K\bar{n}$, where K is a threshold parameter and $\bar{n}$ is the average magnitude of the filtered noise. The average noise level $\bar{n}$ probably influences signal detection more than the threshold parameter because its values for different optical sensors and electronic filters can differ by as much as 20 dB. The threshold parameter's range is smaller unless the clutter-edge effect described in section IIB is extreme. If $\bar{n}$ is fixed by specifying the optical sensor and electronic filter, the quality of signal detection then depends on the threshold parameter and the excursions of the filtered noise magnitude about its average. These excursions are due to ordinary statistical variations and to non-stationarity. A 1-D adaptive threshold sensor samples the filter output and averages the magnitudes of 2n sampled values x_f which lie equally about a single value x_w whose signal content is to be tested. The average $\langle |x_f| \rangle$ is multiplied by a threshold parameter K, and the tested value is declared to be a signal if it exceeds the local threshold $K\langle |x_f| \rangle$. K is chosen to provide a specified false alarm rate. For zero-mean filter output, the average of the 2n magnitudes is a statistical estimate $\hat{n} = \langle |x_f| \rangle$ of the mean absolute deviation $n = \langle |x| \rangle$ of the local noise. The estimate $\hat{n}$ and the threshold $K\hat{n}$ vary as the sampled filter output passes stepwise through the threshold sensor. The distribution of $\hat{n}$ about n is known as the sampling distribution; its standard deviation (s.d.) is called the standard error of the mean, but we will use the simpler names, sampling s.d. and sampling variance. The part of the threshold sensor containing the tested value will be called the signal window, and the part containing the 2n averaged magnitudes will be called the frame.

This summary of the adaptive threshold sensor's operation implies certain effects which occur as the frame size is increased. When the frame is small some estimates of η are much too small, others much to great. Large $\hat{\eta}$ degrade signal detection locally by causing the local threshold to be larger than necessary to prevent false alarms. Small $\hat{\eta}$ degrade signal detection globally since the threshold parameter, which is the same throughout the scene, must be large to prevent false alarms where $\hat{\eta}$ is small. As the frame size is increased the estimates of η become more accurate, the sampling variance and the threshold parameter decrease, and signal detection improves, provided the noise is stationary. If the noise is non-stationary the sampling variance may still decrease with increasing frame size, but the threshold parameter may decrease or increase, and signal detection may improve or deteriorate depending on other factors. To transform this qualitative description into a semi-quantitative one, we analyzed the threshold sensor's sampling performance, related that to the threshold parameter required for a given false alarm rate, and finally linked the threshold parameter to signal detection.

A. Numerical Analysis of Sampling

Sampling of a time series by an adpative threshold sensor can be related computationally to a simple statistical theorem. If random samples of $2n = N$ values each are taken from a data set (population) of more than $20N$ uncorrelated values, the relation between the sampling s.d. $\sigma_{\hat{\eta}}$ and the standard deviation σ of the population is

$$\sigma_{\hat{\eta}}^{\,2} = \sigma^2/N \quad \text{or} \quad \log(\sigma_{\hat{\eta}}/\sigma) = -\log\sqrt{N}. \tag{1}$$

The latter equation is represented by the diagonals in Figure 1. The sampling s.d. is divided by the population s.d. to facilitate comparison of results from data sets with different variances. It is useful to think of a one-sided threshold sensor and consider the limit of equation (1) when $N = 1$. In that case $\hat{\eta} = |x_f|$ so that $\sigma_{\hat{\eta}} = \sigma$ by definition, and the equation is an identity. Thus, we expect equation (1) to be nearly satisfied when the sample size is small, regardless of other conditions. Except for $N = 1$, however, the theorem is not applicable to the adaptive threshold sensor and the recorded background noise because the threshold sensor does not take random samples and the recorded noise is correlated and non-stationary. To relate the statistical theorem to the problem in hand, we made computations in which we first approximated the conditions of the theorem and then relaxed them by steps to arrive at the actual conditions.

Nine segments of uncorrelated, Gaussian, pseudo random noise were generated by the method described in reference 2. This was done for two segment lengths, 1900 values and 3200 values, which are the average lengths of the segments of recorded uniform sky noise and of clutter used in the first article. Sampling variances were calculated by passing the segments

through the adaptive threshold algorithm using ten frame sizes from 8 to 640 values. The results appear in Figures 1(A) and 1(B), where the dots indicate the sampling s.d.s for the whole data set, and the bars span the ranges of the sampling s.d.s for the segments. (A population sampling variance is the average of the associated segment sampling variances.) The sampling s.d.s for the population are on or very near the diagonals showing that sampling by the adaptive threshold sensor is equivalent to random sampling if the noise is stationary and uncorrelated. The ranges of the sampling s.d.s for the segments result from ordinary statistical differences between the segments. They are larger for the shorter segments as expected.

Next the synthetic noise was passed through the 1-D LMS filter to obtain Gaussian noise with the same correlation as the LMS-filtered uniform sky noise. The correlated synthetic noise was then processed in the same way as the uncorrelated noise; results are plotted in Figures 1(C) and 1(D). Correlation reduces the number of independent data in the segments and the frame, so that the values and usually the ranges of the sampling s.d.s are increased. For reasons already given the sampling s.d.s at a frame size of eight data are closer to the diagonals than those at larger frame sizes, which alone are of practical importance. At the larger frame sizes correlation simply shifts the reference line rightward parallel to itself, as illustrated by the lines with slope −1 drawn through the points at frame sizes above eight.

Finally, sampling variances were calculated for ten segments of uniform sky noise (each 1900 values long) and ten of clutter (each 3200 values long). Comparing these results − Figures 1(E) and 1(F) − with those for correlated synthetic noise, we see that non-random sampling and non-stationarity increase the ranges of the sampling s.d.s and the slopes of the lines through

13

them, most obviously in the case of the clutter. The sampling s.d.s of both the uniform sky noise and the LMS-filtered clutter can be described empirically at the frame sizes of interest simply by extending equation (1) to include the effects of non-random sampling, correlation, and non-stationarity. The general equation for any line in Figure (1) is

$$\log (\sigma_{\hat{\eta}}/\sigma) = \beta + \alpha \log \sqrt{N}. \tag{2}$$

The line through the uniform sky results is adequately fit by $\alpha = -0.909$ and $\beta = 0.0819$, that through the clutter results by $\alpha = -0.530$ and $\beta = -0.0433$.

The fact that $\alpha > -1$ for the uniform sky results requires comment. The uniform sky noise may not be strictly stationary because small gain differences ($< 8\%$) between the segments were not corrected. (Neither were they corrected for the simulations here or in the first article.) On the other hand, non-stationarity between segments should increase the ranges of the sampling s.d.s primarily, whereas non-stationarity within the segments should be the chief cause of increases in the slopes. The small difference between -1 and α for the uniform sky results may, therefore, be due to ordinary experimental uncertainty like that in Figures 1(A) and 1(C), not to gain differences.

If the noise is stationary, β can be related to the fraction f of the data which are effectively independent. The lines through the sampling s.d.s of the correlated Gaussian noise have $\alpha = -1$ and $\beta = 0.188$. From the latter we find f = 0.42. Calculations of correlation coefficients show that the first and last of five sequential magnitudes in the LMS-filtered synthetic noise are uncorrelated, giving f = 0.40. The theoretical correlation length of LMS-filtered white noise[3] gives f = 0.5 approximately.

Clearly the suggested interpretation of β is sound for correlated stationary noise. If the noise is correlated and non-stationary, β is determined by these two properties jointly, and a numerical analysis would require calculations with synthetic noise having known amounts of each property. The effort did not seem worthwhile. In this case we simply regard equation (2) as an empirical relation useful for interpreting and predicting the effects of changing threshold-sensor size.

B. Threshold Parameter, Critical Sample Size, and Clutter-edge Effect

The sampling s.d.s of the uniform sky and clutter populations are replotted against frame size in Figure 2(A). Obviously in both cases the sampling s.d. decreases at a decreasing rate with increasing frame size. This is not surprising; the law of diminishing returns with respect to sample size is well known. More important is the relation between the sampling s.d. and the threshold parameter. To study this we calculated threshold parameter ratios $x_w/<|x_f|>$ from the two data sets (containing 114 segments each) used in the first article, not from the restricted sets used here to analyze sampling. The frame sizes employed were $2n = 36, 80, 144,$ 240, and 340 data, the limit of 340 being necessary to avoid excessive loss of ratios. This frame size is 23 percent of the smallest segment, which means that 23 percent of the data in that segment cannot be used as window values x_w. If larger frame sizes were used with the segmented data, the results would be unreliable because of the additional ratios lost.

Figure 2(B) shows threshold parameters which allow one false alarm (f.a.) in all the data or one in the uniform sky. The one false alarm permitted in all the data always occurs in the clutter. Except for a clutter-edge effect discussed below, the threshold parameter behaves as the sampling s.d. does. This means that there are certain "critical sample sizes" beyond which the threshold parameter decreases and (looking ahead) signal detection improves very slowly. The critical sample size depends on the fractional rate of decrease of the sampling s.d., which is obtained by differentiating equation (2).

16

$$\frac{1}{(\sigma_{\hat{\eta}}/\sigma)} \frac{d(\sigma_{\hat{\eta}}/\sigma)}{dN} = \frac{\alpha}{2N} \qquad (3)$$

If F is the fractional rate of decrease at the critical sample size N_c, then $N_c = \alpha/2F$. From Figures 2(A) and 2(B) the critical sample size in uniform sky appears to be about 250 data, so that $F \sim 1.8 \times 10^{-3}$ per datum. Owing to the clutter-edge effect, it is difficult to estimate the critical sample size in clutter from Figure 2. However, if F has the same value in clutter as in uniform sky, then $N_c \sim 150$ data (6 milliradians) in clutter, which agrees well enough with the appearance of the curves. The critical sample size is always greater in uniform sky than in clutter, provided F is the same in the two regions, because $|\alpha|$ is always greater in uniform sky than in clutter.

The plot of sampling s.d. in clutter suggests that the threshold parameter for one f.a. in clutter should decrease slowly beyond $N_c = 150$ data. In fact, it passes through a broad, shallow minimum because of the following "clutter-edge effect," which appears to begin at a frame size between 8 and 10 milliradians (200 and 250 data). As the size of the threshold sensor is increased, the frame includes larger and larger proportions of the benign clutter which flanks severe clutter like that in Figure 4(C) of the first article. This lowers the estimates $\hat{\eta} = \langle |x_f| \rangle$ and raises the threshold ratios $x_w/\hat{\eta}$ in the vicinity of the severe clutter, thus increasing the threshold parameter. Ordinarily the increase will be no more than a few decibels; only an extreme clutter-edge effect like the hypothetical one described in section VB of the first article could change

17

the threshold parameter by 10-20 dB. (Partly for this reason, the threshold sensor usually affects signal detection less than the optical sensor and electronic filter, as noted earlier.) Here the increase - 2.3 percent between frame sizes of 240 and 340 data - is within the experimental uncertainty. However, the occurrence of a clutter-edge effect fits so well into the pattern of the results that we do not doubt its actuality. With that granted the dashed part of the top curve in Figure 2(B) indicates how the threshold parameter might behave at larger frame sizes.

To verify or refute this behavior would require computations with unsegmented data. Many frame size effects can be studied without separating uniform sky noise from clutter, and in some respects it would be better not to separate them. If the data were not segmented, much larger frame sizes could be used before the loss of window values mentioned above became a problem. This would be advantageous for frame size studies, but would hide differences between performance in uniform sky and clutter. We chose to emphasize the latter, realizing that frame size studies with separated data are valid provided the clutter segments do not begin or end at clutter edges, a condition satisfied here.

(The clutter-edge effect has also been called the "cloud-edge" effect, but bright cloud edges may not be its only cause. The term, "clutter-edge," is preferable since it accurately describes the origin of the effect in the waveform but is noncommittal about its origin in the scene.)

18

C. Signal Detection, Optimum Sample Size, and Best Sample Size

Frequencies of detecting simulated signals were calculated using the
threshold parameters in Figure 2(B) and the two data sets of 114 segments
each from uniform sky and from clutter. The results are plotted in Figure 3
except those for the frame size of 144 data, which are in the first article.
From these curves we obtained data for Figure 4, where simulated signal
strengths required for detection frequencies of 0.50, 0.70, 0.90, and 0.95 are
plotted against frame size. The ordinates of curves in Figure 4 will be
called "equally detected signal strengths."

The curves of equally detected signal strengths are much like the top
threshold parameter curve in Figure 2(B), indicating that the threshold-
sensor size affects signal detection chiefly through its effect on the
threshold parameter. The minima of the curves occur, regardless of
detection frequency, at a frame size of about 10 milliradians (250 data),
the same as the minimum of the threshold parameter curve. This is the
optimum sample size for signal detection. Increasing the frame size to
14 or 15 milliradians increases equally detected signal strengths about
0.2 dB, the same as the causative increase of the threshold parameter.
Because of the scales employed in Figure 4, signal detection appears to
deteriorate quickly below the optimum size, but actually it does not. Using
frames of 36 or 144 data rather than the optimum size reduces signal
detection by only 2.4 dB or 0.2 dB respectively. Thus, with a 1-D LMS
filter the best sample size is the critical sample size in clutter since
use of a larger frame risks a clutter-edge effect but improves signal detec-
tion very little in either clear sky or clutter. The frame must not be too
much less than the optimum size, however, because the curves in Figures 2(B)
and 4 are rising rapidly at 36 data, one-seventh the optimum size.

19

III. Summary and Conclusions

We first summarize results and state conclusions which are valid in general for an adaptive threshold sensor following a spatial filter. Barring an extreme clutter-edge effect, the quality of signal detection depends primarily on the average magnitude of the filtered noise (set by the optical sensor and spatial filter) and secondarily on the threshold parameter. The threshold parameter required for a given false alarm rate is determined by the threshold sensor's sampling variance and by a clutter-edge effect. Sampling variance decreases at a decreasing rate with increasing threshold-sensor (sample) size. The decrease is more rapid when the sampled noise is stationary than when it is non-stationary. There are loosely delimited critical sample sizes above which sampling variance decreases very slowly. The critical sample size is larger for stationary than for non-stationary noise. Above the critical sample size in clear sky, the threshold parameter and equally detected signal strength also decrease very slowly. They behave similarly in clutter, provided there is no clutter-edge effect. If there is one the behavior depends on the relation between the threshold-sensor size at which it begins and the critical sample size in clutter. If the two sizes are about the same, the threshold parameter and equally detected signal strength each have a narrow minimum. If the edge-effect onset is larger than the critical sample size, the minima are broad, as in Figures 2(B) and 4. Whether the minima are shallow or deep depends on the magnitudes of the sampling variance effect and the clutter-edge effect. Ordinarily these factors change the threshold parameter and signal detection no more than few decibels within the range of practical threshold-sensor sizes. Only an extreme clutter-edge effect could result in changes greater than 10 dB.

The foregoing summary makes the following useful principle self-evident: If the onset of the clutter-edge effect with a 1-D threshold sensor is less than the critical sample size in either clutter or clear sky, a 2-D threshold sensor may be advantageous, otherwise it will not be. To apply this principle, one must know the critical sample sizes and the onset of the clutter-edge effect. The critical sample sizes can be estimated from the sampling variance, the threshold parameter, or signal detection. The sampling variance gives the least accurate estimates but is by far the easiest method to use. A weak clutter-edge effect and its onset can be found only from the threshold parameter or signal detection; perhaps a stronger one could also be found from the sampling variance.

We next summarize less general results and conclusions. These are valid only for a 1-D adaptive threshold sensor following a 1-D LMS filter 0.3 mR (7 data) long when the filter input is from an optical sensor having an NEI greater than 1.5×10^{-13} W/cm^2 and a spatial resolution better than 0.15 x 0.36 mR. Further restrictions are imposed by the man-made and natural conditions under which the background data were recorded, sampled, and digitized as described in the first article.

Under the stipulated conditions the critical sample size is 10 mR (250 data) in uniform sky and 6 mR (150 data) in clutter. A clutter-edge effect with an onset between 8 and 10 mR results in an optimum threshold-sensor size of 10 mR, but increasing the size to 14-15 mR increases the threshold parameter and equally detected signal strengths only 0.2 dB, indicating a very weak clutter-edge effect. (The weakness is due to the fact that the worst clutter in the filtered data is the same order of magnitude as the NEI.) Similarly, the threshold sensor can be

21

made smaller than the optimum size with very little loss of signal detection; for example, the loss is only 0.2 dB at the critical sample size in clutter. Consequently, the best 1-D threshold-sensor size is the critical sample size in clutter because the larger optimum size risks a clutter-edge effect but improves signal detection very little. Finally, a 2-D threshold sensor probably would not be advantageous in this case since the critical sample size can be reached with a 1-D threshold sensor in both clutter and uniform sky with no significant loss of signal detection owing to the clutter-edge effect.

References

1. M. S. Longmire, A. F. Milton, and E. H. Takken, Appl. Opt. 21, 3819 (1982).

2. D. E. Knuth, The Art of Computer Programming (Addison-Wesley, Reading, MA, 1981), 2nd ed., vol. 2, p. 117.

3. E. H. Takken, D. Friedman, A. F. Milton, and R. Nitzberg, Appl. Opt. 18, 4220 (1979).

Figure 1. Sampling standard deviation (s.d.) of average noise magnitude

estimates $\hat{\eta}$ as a function of threshold-sensor sample size,

noise type, and segment length. The sample sizes are 8, 18,

36, 80, 144, 240, 340, 440, 540, and 640 data. Noise data of

each type are divided into segments of the specified lengths.

There are 9 segments in each of the data sets (A)-(D), and 10

segments in each of the sets (E)-(F). Variances are calculated

about the average magnitude η of all data in a set. Bars show

the ranges of the sampling s.d.s of the segments; dots indicate

the sampling s.d. of the population (all segments of the set).

A population sampling variance is equal to the average of the

associated segment sampling variances. Sampling s.d.s $\sigma_{\hat{\eta}}$ are

divided by the associated population s.d. σ to facilitate

comparison of results from different data sets. The diagonals

represent the logarithmic form of equation (1). The lines

through the dots of data sets (C)-(F) are drawn for best visual

fits.

(A) UNCORRELATED GAUSSIAN NOISE — SEGMENT LENGTH = 1900 NOISE VALUES
(B) UNCORRELATED GAUSSIAN NOISE — SEGMENT LENGTH = 3200 NOISE VALUES
(C) CORRELATED GAUSSIAN NOISE — SEGMENT LENGTH = 1900 NOISE VALUES
(D) CORRELATED GAUSSIAN NOISE — SEGMENT LENGTH = 3200 NOISE VALUES
(E) UNIFORM SKY NOISE — SEGMENT LENGTH = 1900 NOISE VALUES
(F) CLUTTER — SEGMENT LENGTH = 3200 NOISE VALUES

FRAME SIZE (Noise Values)
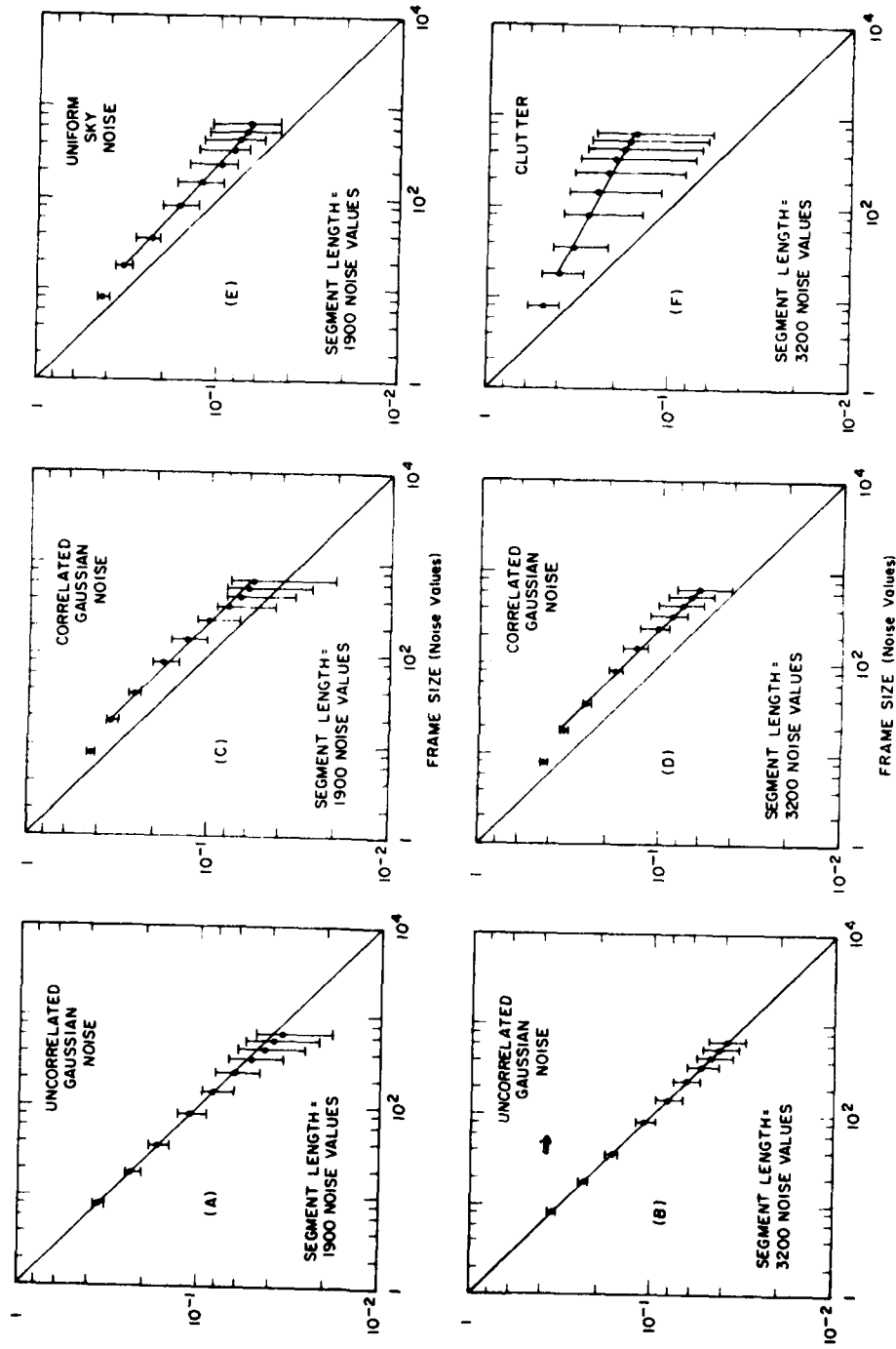
SAMPLING S.D., q/σ (Units of Population S.D.)

Figure 2. Sampling standard deviation (s.d.) and threshold parameter K
as functions of threshold-sensor sample size and noise type.
The sample sizes are 36, 80, 144, 240, and 340 data. (A) Pop-
ulation sampling s.d.s for the data sets of Figures 1(E) and
1(F); each set contains 10 segments. (B) Threshold parameters
for one false alarm (f.a.) determined from the two data sets
in reference 1; each set contains 114 segments.

FRAME SIZE (mR)

(B)

I F.A. IN CLOUDS & IN WHOLE SCENE

HYPOTHETICAL
CLUTTER–EDGE EFFECT

CLUTTER–EDGE EFFECT

I F.A. IN UNIFORM SKY ALONE

THRESHOLD PARAMETER

8.00

7.00

6.00

5.00

FRAME SIZE (Noise Values)

(A)

BACKLIT CLOUDS

UNIFORM SKY

SAMPLING S.D., $\sigma_{\bar{x}}/\sigma$ (Units of Population S.D.)
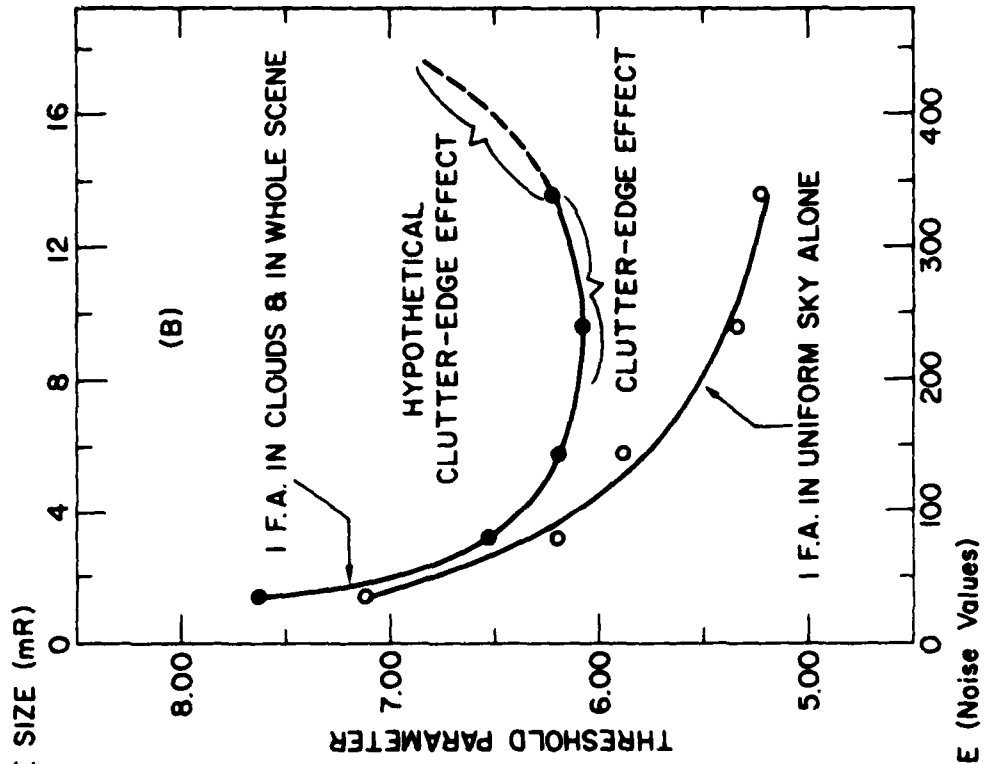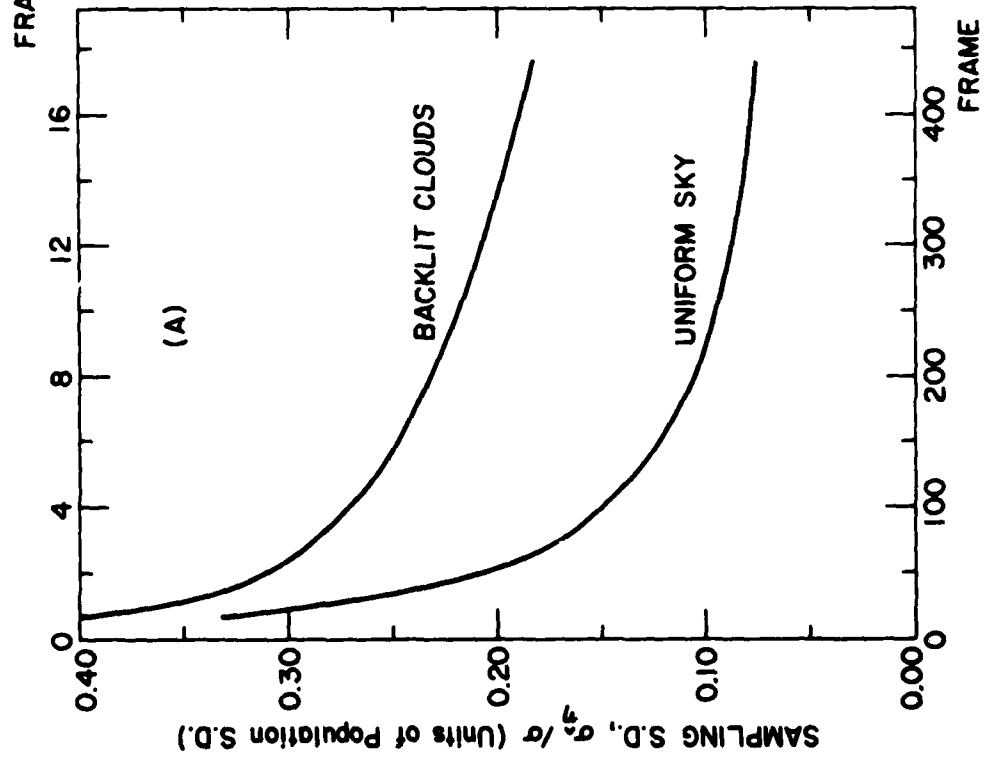
0.40

0.30

0.20

0.10

0.00

Figure 3. Frequencies of detecting simulated signals in LMS-filtered

natural background noise with threshold sensors of different

sizes. These results are calculated from the two data sets

used in reference 1; each set contains 114 segments. Results

for a frame size of 144 data are in reference 1. The threshold

parameters for one false alarm (f.a.) are plotted in the top
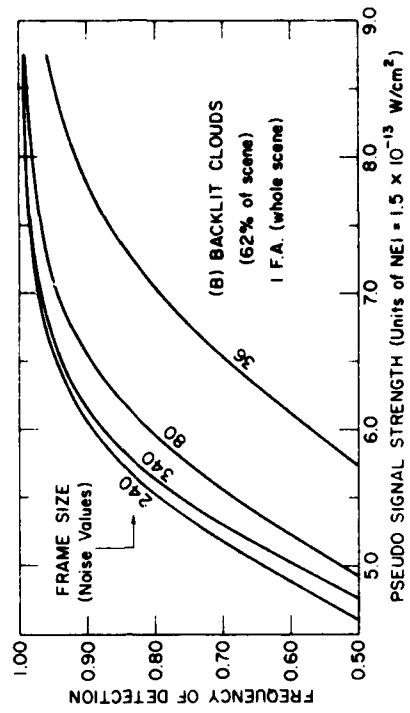
curve of Figure 2(B).

(A) UNIFORM SKY
(38% of scene)
1 F.A. (whole scene)

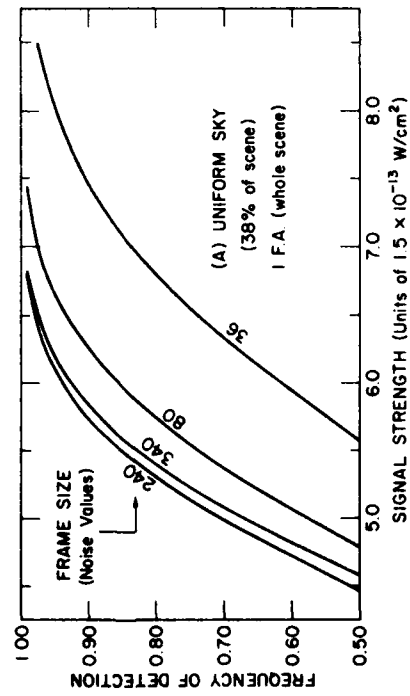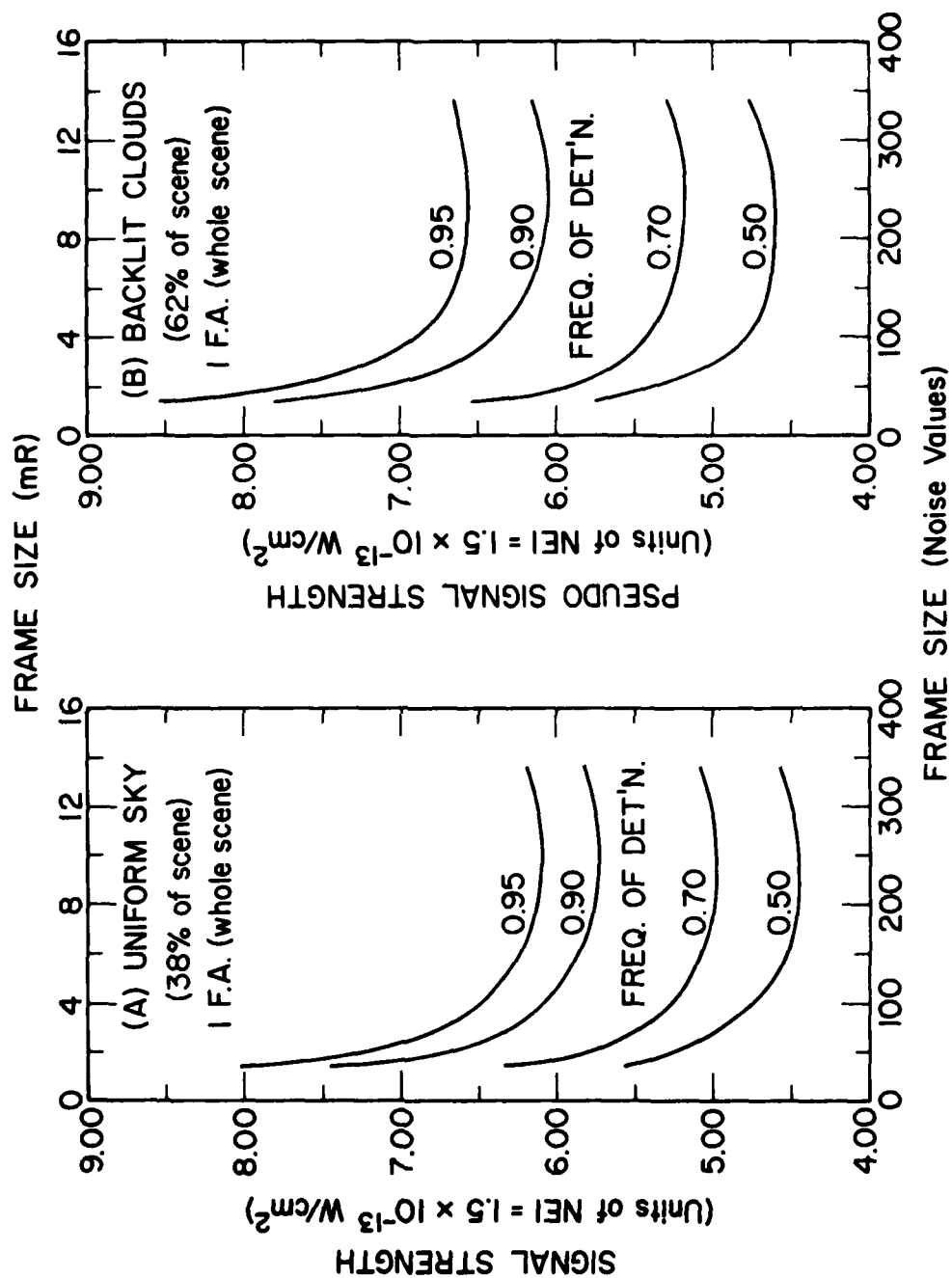(B) BACKLIT CLOUDS
(62% of scene)
1 F.A. (whole scene)

Figure 4. Equally detected signal strength as a function of threshold-
sensor size, noise type, and detection frequency. Simulated
signal strengths for these plots were read from the curves in
Figure 3. The curves here show simulated signal strengths
required to achieve the indicated detection frequencies with
threshold sensors of different sizes.

FRAME SIZE (mR)

(B) BACKLIT CLOUDS
(62% of scene)
I F.A. (whole scene)

0.95
0.90
FREQ. OF DET'N.
0.70
0.50

PSEUDO SIGNAL STRENGTH
(Units of NEI = 1.5 × 10⁻¹³ W/cm²)

$PSEUDO\ SIGNAL\ STRENGTH$ (Units of NEI = 1.5×10^{-13} W/cm²)

FRAME SIZE (Noise Values)

(A) UNIFORM SKY
(38% of scene)
I F.A. (whole scene)

0.95
0.90
FREQ. OF DET'N.
0.70
0.50

SIGNAL STRENGTH
(Units of NEI = 1.5×10^{-13} W/cm²)

PART 4

Data for Simulation of 2-D Signal Processing

The work reported in Parts 1 and 3 has shown that high spatial

resolution, one-dimensional (1-D) spatial filtering, and 1-D adaptive

threshold sensing are an effective combination for suppressing extreme cloud

clutter and detecting signals from point sources in either clear sky or cloud

clutter when the NEI of the surveillance system is greater than 10^{-13} W/cm^2.

At the same time it was found that, even with very good spatial resolution,

the worst clutter from backlit clouds passes a 1-D LMS spatial filter at a

level of 5-6 x 10^{-13} W/cm^2, which apparently is the clutter rejection limit

of 1-D signal processing techniques. If the system NEI were lower, this

leakage of extreme clutter would limit the expected improvement of signal

detection in clear sky and benign clutter. Further clutter rejection is thus

desirable; perhaps it could be obtained by two-dimensional (2-D) signal

processing -- that is, by processing inputs from several detector elements

(channels) to produce a single channel of output. Two-dimensional filtering

will reduce clutter leakage if the clutter outputs of 1-D LMS filters are

correlated in the cross-scan direction. Two-dimensional adaptive threshold

sensing will be advantageous if the residual clutter occurs in isolated small

patches several times larger than the optical blur circle.

The data employed for the work reported in Parts 1 and 3 are unsuitable

for studies of 2-D signal processing on two accounts. First, they show no

channel-to-channel correlation or isolated small clutter patches. Second,

they contain only six channels, too few for 2-D simulations. At least

three -- more likely five -- channels of input are required for a single
channel of output from a 2-D filter or threshold sensor. If five channels of
input are required, about eight channels of data are needed to simulate the
performance of either a 2-D filter or a 2-D threshold sensor, and about
twelve channels are needed to simulate the performance of a 2-D threshold
sensor following a 2-D filter.

An effort was made to obtain suitable data through an exchange arranged
by the Naval Air Development Center, Warminster, PA, and the Canadian Defense
Research Establishment Valcartier, Quebec. Data gathered under sponsorship
of the Naval Research Laboratory were traded for data collected by French
workers. The terms of the exchange required all data to be supplied on
magnetic tape in a standard NATO format. Computer programs for reading and
writing the NATO-format tapes were developed by the Control Data Corporation
(CDC) with the assistance of the project director for this contract. The
FORTRAN V program which reads NATO tapes and reformats the contents for use
on the CDC Cybernet system is stored on tape A07739 at the Eastern Cybernet
Center in Rockville, MD. This tape also has the French data reformatted for
use on the Cybernet system.

Parameters characterizing the French data are given in Table 4.1, where
important missing information is also indicated. Certainly there are
sufficient channels for 2-D simulations, but examination of the table reveals
the following difficulties.

1. More information about the layout of the detector elements in the array
   is needed before the spatial resolution of the data can be reduced to
   simulate optical sensors with larger instantaneous fields of view.

2. Simulations with these data cannot be fully interpreted and related to
   simulations with other data unless the NEI at the output of the data
   collection filter is known.

29

3. The sampled azimuthal field-of-view is barely large enough for simulating adaptive threshold sensors. One twice as large would be better.

4. The point spread function (detector output from a point source) must be known in order to derive weights for simulating matched filters and also to reduce the spatial resolution of the data.

5. The high frequency cut-off of the data collection filter is less than half that of the optical sensor's point source output. Consequently, simulations with these data will be strongly affected by the properties of the data collection filter. This means that the data cannot be used to study processing of the optical sensor's output, which is the type of study usually desired.

6. Recording the data should not affect its properties. For that reason it would be reassuring to know the tape recorder's characteristics, especially those listed, even though this information is not essential for simulations.

7. The sample time (time to take a sample of the electrical filter output) must be known in order to derive suitable weights for simulating digital filters. This is especially important here since the number of samples per dwell is small.

8. Eight bits do not provide enough range for extreme cloud-clutter data if they are recorded and digitized on linear scales. If the scales are not linear, they must be known before the data can be used.

Among these difficulties only one, the cut-off frequency of the electrical filter, is necessarily fatal to the intended use of the data. The choice of a filter cut-off less than the point-source cut-off is unusual for data collection and invites inquiry about the reason for it. Perhaps the data were not collected for general use in simulations but for development of

a particular device having a cut-off (or scaled cut-off) the same as that employed. Alternatively, the reported cut-off may be in error, although this seems unlikely since it is given as both a temporal and a spatial frequency, and the two agree. Nevertheless, further inquiries about the electrical filter cut-off should be made because the data cannot be used for general simulations if the value in Table 4.1 is correct.

Table 4.1.   Parameters for Recording French Data

Spectral Bands	2.8–5.6 µm and 7.2–11.2 µm
Detector Array	288 elements, 144 in each spectral band. No more information presently available.
NEI at Output of Data Collection Filter	?
Field of View	Each element (resolution): 0.25 mR (az) x 0.25 mR (el) Total 360° (az) x 2° (el) = 6283 mR (az) x 34.9 mR (el) Sampled 81.8 mR (az) x 34.9 mR (el)
Detector Output from a Point Source	?
Scan	Rate: 360°/1.33 s = 4724 mR/s Dwell time = 5.3×10^{-5} s Point source cut-off ≈ 9450 Hz
Electrical filter	20–3800 Hz passband
Tape Recorder	Bandwidth = ? Dynamic range = ? Noise level ÷ NEI = ?
Sampling	Azimuthal sampling interval 0.16 mR or 3.4×10^{-5} s Sampling rate 1.56/dwell or 29,500/s Sample time = ?
Digitization	Sign bit and 7 numeric bits = $\pm$ 128 full scale

32

FIL